

Theoretical Insights into C–H Bond Activation of Methane by Transition Metal Clusters: The Role of Anharmonic Effects

Preeti Bhumla,* Manish Kumar, and Saswata Bhattacharya*

Department of Physics, Indian Institute of Technology Delhi, New Delhi, India

E-mail: Preeti.Bhumla@physics.iitd.ac.in[PB]; saswata@physics.iitd.ac.in[SB]

Phone: +91-11-2659 1359. Fax: +91-11-2658 2037

Supplemental Material

- I. Comparison of functionals (PBE and HSE06) in finding global minimum structures
- II. Temperature control using Nose-Hoover thermostat
- III. Contribution of F_{vib} in all Ni-based clusters at different temperatures
- IV. Thermodynamic integration for Helmholtz free energy evaluation
- V. Probability of occurrence of different type of configurations

I. Comparison of functionals (PBE and HSE06) in finding global minimum structures

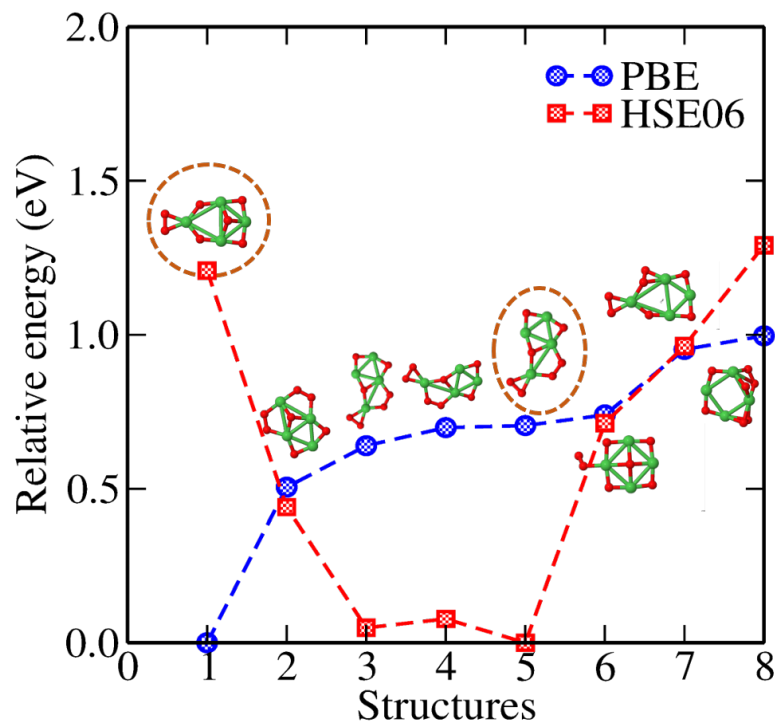


Figure S1: Structures of different isomers of Ni_4O_7 clusters obtained from PBE (represented by dashed blue line) and HSE06 (represented by dashed red line) exchange-correlation (ϵ_{xc}) functionals. Dashed circles represent the global minima from the two functionals.



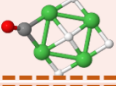
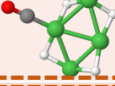
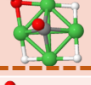
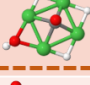
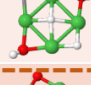
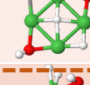
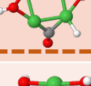
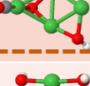
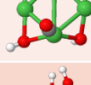
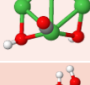
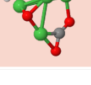
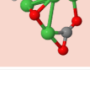
Clusters	PBE	HSE06
Ni_4CH_4		
$\text{Ni}_4\text{O}_1\text{CH}_4$		
$\text{Ni}_4\text{O}_2\text{CH}_4$		
$\text{Ni}_4\text{O}_3\text{CH}_4$		
$\text{Ni}_4\text{O}_4\text{CH}_4$		
$\text{Ni}_4\text{O}_5\text{CH}_4$		
$\text{Ni}_4\text{O}_6\text{CH}_4$		

Figure S2: Global minimum structures of $\text{Ni}_4\text{O}_x\text{CH}_4$ clusters obtained from PBE and HSE06 ε_{xc} functionals. Dashed rectangle indicates the clusters having different global minima.

We have determined the energy of different isomers of Ni_4O_7 clusters from both the ε_{xc} functionals viz. PBE¹ and HSE06.² From Figure S1, we have found that PBE ε_{xc} functional predicts structure 1 as the global minimum isomer while structure 5 is the global minimum isomer obtained from HSE06 ε_{xc} functional. Further, we have calculated the energy of $\text{Ni}_4\text{O}_x\text{CH}_4$ ($0 \leq x \leq 6$) series of clusters from PBE as well as HSE06 ε_{xc} functionals (see Figure S2). We have noticed different trends of energy from both functionals. For $\text{Ni}_4\text{O}_1\text{CH}_4$, $\text{Ni}_4\text{O}_2\text{CH}_4$ and $\text{Ni}_4\text{O}_4\text{CH}_4$ clusters, PBE and HSE06 ε_{xc} functionals predict different global minimum structures. As it is already well established that for oxygen molecule, HSE06 being advanced functional gives correct binding energy,³ therefore, we have chosen HSE06 for our oxide based clusters.

II. Temperature control using Nose-Hoover thermostat

We have carried out *ai*MD simulations at five different temperatures in canonical ensemble with time and time-step being 8 ps and 1 fs, respectively. Temperature control is realized by employing the Nose-Hoover thermostat.⁴ Figure S3 shows the histogram that we have obtained from *ai*MD simulation for Ni₄O₆CH₄ cluster at $T = 800$ K. From the histogram, we infer that average temperature of the simulation is indeed coming around the intended temperature viz. 800 K. Therefore, Nose-Hoover thermostat is apt to control the temperature during simulation. Note that thermalization of system is very important and without that there is sufficient chance of error. However, once the system is well thermalized at the target temperature T , we can expect reasonably same numbers for $\langle U \rangle_T$ and $\langle T \rangle$ (see equation 1) from the residual run (not much of dependence on the length of the run within reasonable error bar).

$$F(T) = \underbrace{E^{\text{DFT}} + U^{\text{ZPE}}}_{U^{\text{ref}}} + \frac{T}{T_{\circ}} F_{\text{vibs}}^{\text{harmonic}}(T_{\circ}) - T \underbrace{\int_{T_{\circ}}^T \frac{dT}{T^2} (\langle U \rangle_T - U^{\text{ref}})}_{\text{thermodynamic integration}} - k_B T \frac{N}{2} \ln \frac{T}{T_{\circ}} \quad (1)$$

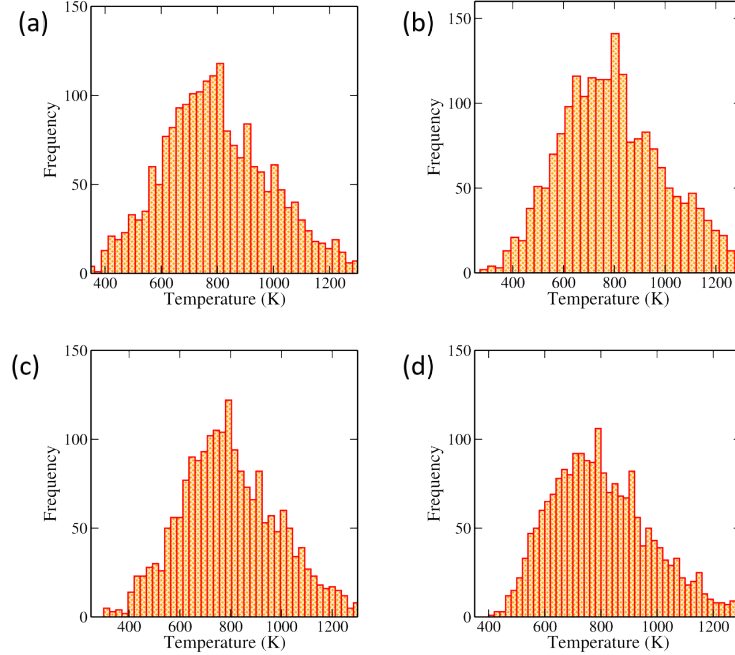


Figure S3: Histogram of $\text{Ni}_4\text{O}_6\text{CH}_4$ configuration at 800 K. The average temperature obtained is (a) 804 K after 4 ps (b) 800 K after 5 ps (c) 801 K after 6 ps (d) 796 K after 7 ps.

Here, we have taken a test case of $\text{Ni}_4\text{O}_6\text{CH}_4$. We have run 8 ps MD and plotted four such histograms, where (a) 4 ps (b) 5 ps (c) 6 ps and (d) 7 ps data are used for thermalization. The remaining (a) 4 ps (b) 3 ps (c) 2 ps and (d) 1 ps are used to plot the figure below. Note that the target T is 800 K and the average $\langle T \rangle$ found from case (a)-(d) are respectively (a) 804 K (b) 800 K (c) 801 K and (d) 796 K. Clearly, here the system is already thermalized at (a) and once it is ensured, the rest of the data remain more or less same to give the same $\langle T \rangle$ within accepted error bar of ± 10 K max. Now time required for thermalization slightly increases with number of atoms. This is why we have kept data for thermalization to be large enough ($\sim 6-7$ ps) and used the residual ($\sim 2-1$ ps) to determine $\langle U \rangle_T$ and $\langle T \rangle$ respectively to ensure error free simulation numbers.

III. Contribution of F_{vib} in all Ni-based clusters at different temperatures.

The total Helmholtz free energy $[F(T)]$ is written as:

$$F(T) = F_{trans}(T) + F_{rot}(T) + F_{vib}(T) + F_{sym}(T) + F_{spin}(T) \quad (2)$$

where F_{vib} is given by the following equation:

$$F_{vibs} = \sum_i \frac{h\nu_i}{2} + \sum_i k_B T \ln \left[1 - \exp\left(-\frac{h\nu_i}{k_B T}\right) \right] \quad (3)$$

To see the comparative contribution of F_{vib} at different temperatures, namely, $T=100$ K, $T=300$ K and $T=800$ K, we have plotted the bar graph as shown in FIG. S4.

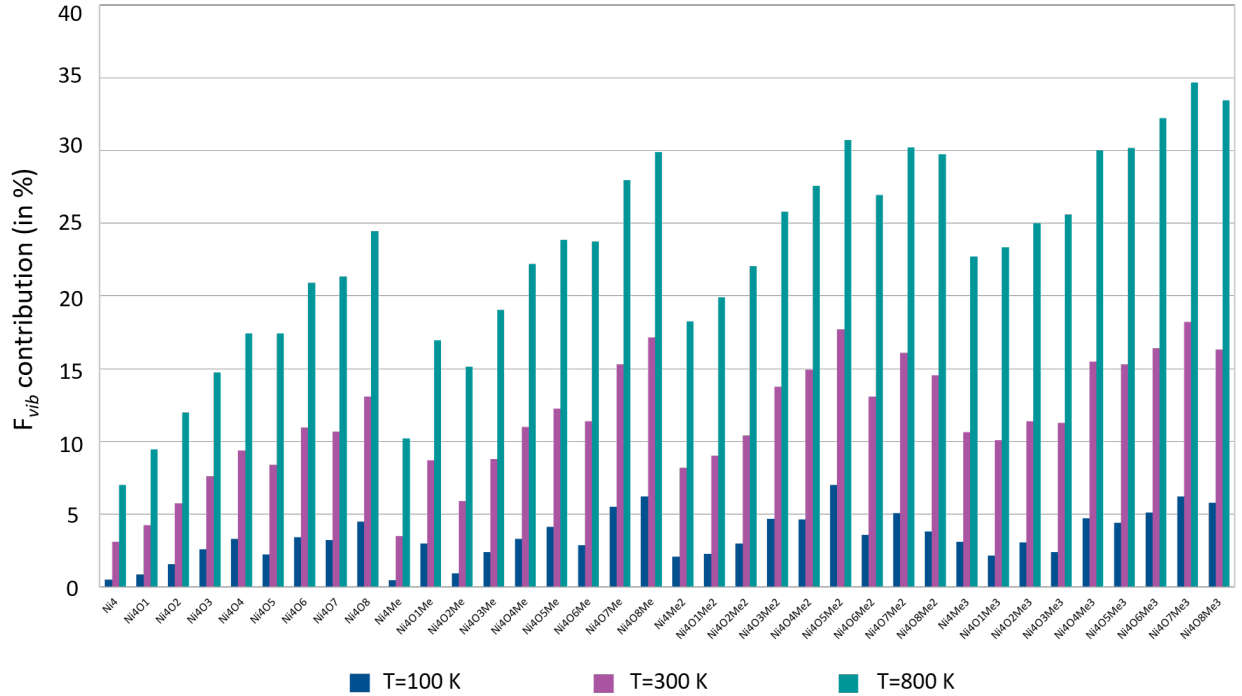


Figure S4: F_{vib} contribution (in %) in all Ni-based clusters at $T=100$ K, $T=300$ K and $T=800$ K, respectively. (Here, Me represents CH_4).

From FIG. S4, we can see that F_{vib} contributes more at higher temperatures.

IV. Thermodynamic integration for Helmholtz free energy evaluation

We start from the fundamental relation between Helmholtz free energy $F(T)$ and partition function Z .

$$F(T) = -k_B T \ln Z = -k_B T \ln \int e^{-\beta H} dp dr \quad (4)$$

where H (i.e., kinetic energy, K , plus potential energy, U) is the Hamiltonian of the system (cluster), and $\beta = 1/k_B T$. This on integration gives us

$$F(T) = -k_B T \ln \int e^{-\beta U} dr + N k_B T \ln \Lambda(T) \quad (5)$$

where N is number of degrees of freedom and $\Lambda(T)$ is the result of integration over momentum space and always valid only if the system is classical. In terms of β , the expression for $\Lambda(\beta)$ is: $\Lambda(\beta) = \sqrt{\frac{h^2 \beta}{2\pi m}}$

Equation 1 can then be written as:

$$\beta F(\beta) = -\ln \int e^{-\beta U} dr + N \ln \Lambda(\beta) \quad (6)$$

$$\frac{\partial[\beta F(\beta)]}{\partial \beta} = \frac{\frac{\partial}{\partial \beta} \int e^{-\beta U} dr}{\int e^{-\beta U} dr} + N \frac{\frac{\partial}{\partial \beta} \Lambda(\beta)}{\Lambda(\beta)} = \langle U \rangle_\beta + \frac{N}{2\beta} \quad (7)$$

$$\beta F(\beta) = \beta_\circ F(\beta_\circ) + \int_{\beta_\circ}^{\beta} \langle U \rangle_\beta d\beta + \frac{N}{2} \int_{\beta_\circ}^{\beta} \frac{\partial \beta}{\beta} \quad (8)$$

Now $F(\beta_\circ)$ can be written as:

$$F(\beta_\circ) = \underbrace{E^{\text{DFT}} + U^{\text{ZPE}}}_{U^{\text{ref}}} + F^{\text{vib}}(\beta_\circ) \quad (9)$$

where from quantum approach, we have

$$F_{quantum}^{vib}(\beta) = \beta^{-1} \sum_{i=1}^N \ln(1 - e^{-\beta h\nu_i}) \quad (10)$$

and from classical approach, we have

$$F_{classic}^{vib}(\beta) = \beta^{-1} \sum_{i=1}^N \ln(\beta h\nu_i) \quad (11)$$

Therefore, we get the final expression of $\beta F(\beta)$ as shown below:

$$\beta F(\beta) = \beta_0 U^{ref} + \beta_0 F^{vib}(\beta_0) + \int_{\beta_0}^{\beta} \langle U \rangle_{\beta} d\beta + \frac{N}{2} \ln \frac{\beta}{\beta_0} \quad (12)$$

We call the above equation as our master equation and we will approximate this equation as given below.

Here, we write $\langle U \rangle_{\beta}$ as follows:

$$\langle U \rangle_{\beta} \rightarrow (\langle U \rangle_{\beta} - U^{ref}) \quad (13)$$

Therefore, on substituting this into Equation 9, we get

$$\beta F(\beta) = \beta_0 U^{ref} + \beta_0 F^{vib}(\beta_0) + (\beta - \beta_0) U^{ref} + \int_{\beta_0}^{\beta} (\langle U \rangle_{\beta} - U^{ref}) d\beta + \frac{N}{2} \ln \frac{\beta}{\beta_0} \quad (14)$$

$$= \beta U^{ref} + \beta_0 F^{vib}(\beta_0) + \int_{\beta_0}^{\beta} (\langle U \rangle_{\beta} - U^{ref}) d\beta + \frac{N}{2} \ln \frac{\beta}{\beta_0} \quad (15)$$

This can be rewritten in terms of $T=1/k_B\beta$ as follows:

$$F(T) = E^{DFT} + U^{ZPE} + \frac{T}{T_0} F^{vib}(T_0) - T \int_{T_0}^T \frac{dT}{T^2} (\langle U \rangle_T - U^{ref}) - k_B T \frac{N}{2} \ln \frac{T}{T_0} \quad (16)$$

V. Probability of occurrence of different type of configuration

If N is the total number of all possible configurations and ΔG_n is the Gibbs free energy of formation of specific type (say n) configuration, then the number of type- n configurations, N_n , as per Fermi-Dirac statistics is given as:

$$N_n = \left(N - \sum_{m \neq n} N_m \right) \frac{1}{e^{\beta \Delta G_n} + 1} \quad (17)$$

where $\beta = 1/k_B T$ and N_m is any other considered configuration type.

Similarly, the number of type- p configurations, N_p , is given as:

$$N_p = \left(N - \sum_{m \neq p} N_m \right) \frac{1}{e^{\beta \Delta G_p} + 1} \quad (18)$$

Rearranging above equations, we get

$$N_n e^{\beta \Delta G_n} + N_n = \left(N - \sum_{m \neq n} N_m \right) \quad (19)$$

$$N_p e^{\beta \Delta G_p} + N_p = \left(N - \sum_{m \neq p} N_m \right) \quad (20)$$

On solving Equation 16 and Equation 17, we get

$$N_n e^{\beta \Delta G_n} - N_p e^{\beta \Delta G_p} + N_n - N_p = N_n - N_p \quad (21)$$

$$N_n e^{\beta \Delta G_n} = N_p e^{\beta \Delta G_p} \quad (22)$$

Finally, we get the following expression

$$\frac{N_n}{N_p} = e^{\beta(\Delta G_p - \Delta G_n)} \quad (23)$$

Similarly, we can write

$$\frac{N_m}{N_n} = e^{\beta(\Delta G_n - \Delta G_m)} \quad (24)$$

On substituting the value of N_m from Equation 21 to Equation 14, we get

$$N_n = \left(N - \sum_{m \neq n} N_n e^{\beta(\Delta G_n - \Delta G_m)} \right) \frac{1}{e^{\beta \Delta G_n} + 1} \quad (25)$$

$$N_n e^{\beta \Delta G_n} + N_n = N - \sum_{m \neq n} N_n e^{\beta(\Delta G_n - \Delta G_m)} \quad (26)$$

$$N_n(1 + e^{\beta \Delta G_n}) = N - \sum_{m \neq n} N_n e^{\beta(\Delta G_n - \Delta G_m)} \quad (27)$$

$$N_n \left(1 + e^{\beta \Delta G_n} + \sum_{m \neq n} e^{\beta(\Delta G_n - \Delta G_m)} \right) = N \quad (28)$$

$$\frac{N_n}{N} = \frac{1}{\left(1 + e^{\beta \Delta G_n} + \sum_{m \neq n} e^{\beta(\Delta G_n - \Delta G_m)} \right)} \quad (29)$$

$$\frac{N_n}{N} = \frac{e^{-\beta \Delta G_n}}{\left(e^{-\beta \Delta G_n} + 1 + \sum_{m \neq n} e^{-\beta \Delta G_m} \right)} \quad (30)$$

Therefore, we get the final expression of probability of occurrence of type-n configurations as follows:

$$\frac{N_n}{N} = \frac{e^{-\beta \Delta G_n}}{1 + \sum_m e^{-\beta \Delta G_m}} \quad (31)$$

References

- (1) J. P. Perdew, K. Burke and M. Ernzerhof, *Phys. Rev. Lett.*, 1996, **77**, 3865–3868.
- (2) J. Heyd, G. E. Scuseria and M. Ernzerhof, *J. Chem. Phys.*, 2003, **118**, 8207–8215.

- (3) S. Bhattacharya, S. V. Levchenko, L. M. Ghiringhelli and M. Scheffler, *Phys. Rev. Lett.*, 2013, **111**, 135501.
- (4) D. J. Evans and B. L. Holian, *J. Chem. Phys.*, 1985, **83**, 4069–4074.